ARTICLE

Uniform B-C-N Ternary Monolayer from Non-Metal Filled g-C_3N_4 Sheet

Na Zhang[a], Xiao-jun Wu[a,b,c*]

a. CAS Key Laboratory of Materials for Energy Conversion and Department of Materials Science and Engineering, University of Science and Technology of China, Hefei 230026, China
b. Synergetic Innovation Center of Quantum Information & Quantum Physics, University of Science and Technology of China, Hefei 230026, China
c. School of Chemistry and Materials Science and Hefei National Laboratory for Physical Sciences at the Microscale, University of Science and Technology of China, Hefei 230026, China

(Dated: Received on April 2, 2014; Accepted on April 28, 2014)

By using first principles calculations, four two-dimensional B-C-N ternary sheets with ordered and uniform element distribution are predicted based on the C, B, or N filled g-C_3N_4 sheet. These B-C-N ternary sheets are metallic except for B_4-C_3N_4 monolayer, which is a semiconductor with an energy band gap of 1.18 eV. In particular, the B_3C-C_3N_4 is a ferromagnetic metal with a net magnetic moment of 0.57 μ_B/cell, which can be used to develop metal-free spintronic device. The calculated formation energy indicates these B-C-N ternary sheets are highly thermal stable. It presents a new route to obtain uniform B-C-N ternary sheet for electronic and spintronic applications.

Key words: Density functional theory, B-C-N ternary monolayer, g-C_3N_4

I. INTRODUCTION

Two-dimensional (2D) materials with single atomic thickness have attracted extensive attention for their unique electronic, optical and planar properties with respect to the bulk materials [1, 2]. In particular, two analogs, *i.e.* graphene characterized as a semi-metal or zero gap semiconductor with unique electronic properties [3−5] and hexagonal boron nitride sheet (*h*-BN) as an insulator with a bandgap larger than 5 eV [6, 7], are expected to play a key role in future nanotechnology as well as to provide potential applications in next generation electronics.

In recent years, the hybrid 2D materials by combining graphene and *h*-BN monolayer, *i.e.* 2D B-C-N ternary sheets, have induced rising interest for their novel electronic and magnetic properties, remarkably different from two pristine hosts [8−16]. For instance, introducing *h*-BN flakes into graphene's framework opens a band gap of graphene, induces magnetism or half-metallicity, makes them suitable for electronic and spintronic applications [11]. Experimentally, there have been some successes in preparing 2D B-C-N compositions [8−10]. Ci *et al.* synthesized large-area atomic layers of B-C-N nanosheets, consisting of hybridized, randomly distributed domains of *h*-BN and C phases with compositions ranging from pure BN to pure graphene [8]. Raidongia *et al.* have obtained B-C-N nanosheets by the reaction of high-surface-area activated charcoal with a mixture of boric acid and urea at 900 °C [9], and Qin *et al.* synthesized $B_{0.38}C_{0.27}N_{0.35}$ compounds with few atomic layers by microwave plasma CVD (MPCVD) [10]. Theoretically, a lot of other B-N-C ternary systems such as BC_2N [12], BC_4N [13], B_3CN_3 [14], $B_3C_2N_3$ [15], have been proposed. However, it is found that most of these ternary systems have strong preferences for much more B−N bonds and C−C bonds compositions and the B-C-N ternary sheet prefers a hybridization of graphene and *h*-BN domains [8]. How to obtain B-C-N ternary monolayer material with uniform or ordered distribution of B, C, and N is still a challenge.

Graphitic carbon nitride (g-C_3N_4) is a stacked two-dimensional sheets of tris-triazine connected via tertiary amines, which is an analogue to graphite with nitrogen substitution. Due to its novel optical and chemical properties, g-C_3N_4 has been demonstrated as a potential candidate for optoelectronic conversion and photocatalytic water splitting [16−23]. Recently, ultrathin g-C_3N_4 sheets with enhanced photoresponsivity and possible magnetism have been reported experimentally, implying the great potential applications of 2D g-C_3N_4 sheet [19, 20]. Compared with graphene in structure, the g-C_3N_4 monolayer is porous sheet with uniform-distributed vacancy at atomic level [24, 25]. Thus, it provides a great potential to filling the pores in g-C_3N_4 sheet with B, C, or N atoms to prepare 2D B-C-N ternary materials with uniform and ordered distribution of B, C, and N elements.

In this work, we predicted four 2D B-C-N ternary materials by filling g-C_3N_4 sheet with C, B, and N atoms. On the basis of first principles calculations, the designed

*Author to whom correspondence should be addressed. E-mail: xjwu@ustc.edu.cn

B-C-N sheets were either metallic or semiconductor. In particular, the B_3C-C_3N_4 sheet was ferromagnetic metal, which can be used for developing metal-free spintronic devices.

II. METHODS

All calculations are performed by using the density functional theory (DFT) method within the Perdew-Burke-Ernzerholf (PBE) generalized gradient approximation (GGA) implemented in Vienna *ab initio* Simulation Package (VASP) [26, 27]. The projector augmented wave (PAW) potential and the plane-wave cutoff energy of 500 eV are used [28, 29]. The periodic boundary condition was applied and we used a vacuum space of 15 Å along the z direction to avoid interactions between two $B_xC_yN_z$-C_3N_4 images in the nearest-neighbor unit cells. When performing the geometric optimization, both the cell shapes and atomic positions are fully relaxed for all considered $B_xC_yN_z$-C_3N_4 frameworks. The Brillouin zone is represented through Monkhorst-Pack special k-point meshes [30] with 5×5×1 and 13×13×1 for the geometry optimization and calculating the density of states. More than 20 K points along each high-symmetry line in the Brillouin zone were used to obtain the accurate band structure. The convergence criteria for total energy and force are set to be 500 eV, 1×10^{-4} eV, and −0.01 eV/Å, respectively. As PBE method always underestimates the band gap, the screened hybrid HSE06 functional method is used to evaluate the band gap of semiconductor systems.

III. RESULTS AND DISCUSSION

We first studied the geometric and electronic properties of the pristine 2D g-C_3N_4 framework. Our g-C_3N_4 model is based on the experimentally well characterized structure as shown in Fig.1(a) [31]. The optimized lattice constant of g-C_3N_4 unitcell is calculated to be 7.14 Å, agreeing with previous studies [24, 25]. The energy band structures with PBE and HSE06 methods indicate that the pristine g-C_3N_4 sheet is nonmagnetic semiconductor. The PBE method presents an underestimated band gap of about 1.25 eV, and this value is 2.71 eV with HSE06 method (Fig.1(b)), which is consistent well with the experimental value (2.7 eV) [31]. The orbital projected DOS analysis shows that the valence band edge is mainly contributed by N2p orbitals, whereas the conducting band edge is mainly contributed by C2p and N2p orbitals.

Next, boron, carbon, or nitrogen atoms are incorporated into the porous pristine g-C_3N_4 sheet to get uniform 2D B-C-N ternary monolayer. Four models with the compositions of B_3C-C_3N_4, B_3N-C_3N_4, B_3-C_3N_4, and B_4-C_3N_4, are designed, as shown in Fig.2. A structure distortion can be found in B_3C-C_3N_4, B_3N-C_3N_4, and B_4-C_3N_4, whereas B_3-C_3N_4 monolayer has an exactly planar structure. The optimized lattice constants are summarized in Table I. These values are slightly larger than that of pristine g-C_3N_4 monolayer.

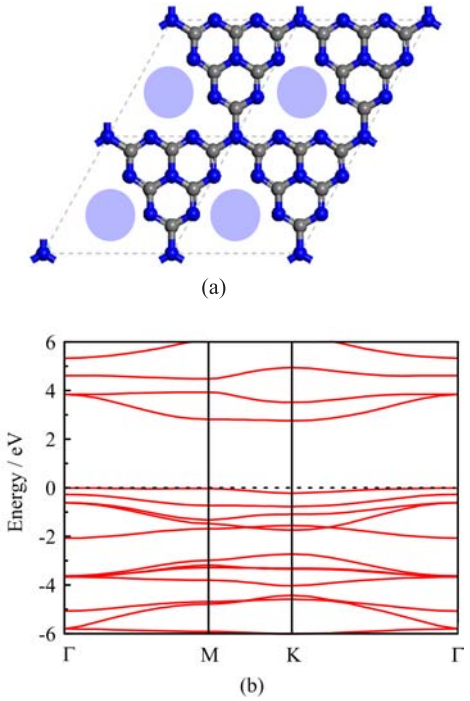

FIG. 1 (a) Geometric structure and (b) band structure of the 2D g-C_3N_4 framework calculated by HSE06. Gray and blue balls represent C and N atoms, respectively.

TABLE I Optimized lattice constant a, binding energy $E_{\rm form}$, total magnetic moment per unit cell M, and band gap $E_{\rm gap}$ of the uniform B-C-N frameworks.

	a/Å	$E_{\rm form}$/eV	$M/\mu_{\rm B}$	$E_{\rm gap}$/eV
g-C_3N_4	7.14	0.294	0.00	2.17
B_3C-C_3N_4	7.27	−0.027	0.57	0.00
B_3N-C_3N_4	7.24	−0.073	0.00	0.00
B_3-C_3N_4	7.24	0.222	0.00	0.00
B_4C-C_3N_4	7.21	0.080	0.00	1.18

To investigate the structure stability of proposed 2D B-C-N ternary monolayer, the average formation energies of pristine g-C_3N_4 and four B-C-N ternary monolayer models are calculated. The formation is defined as

$$E_{\rm form} = \frac{E_{\rm tot} - n_{\rm B}\mu_{\rm B} - n_{\rm C}\mu_{\rm C} - n_{\rm N}\mu_{\rm N}}{n_{\rm B} + n_{\rm C} + n_{\rm N}} \quad (1)$$

where $E_{\rm tot}$ are the total energies of pristine g-C_3N_4 or B-C-N ternary monolayer. The $n_{\rm B}$, $n_{\rm C}$, $n_{\rm N}$ are the total number of B, C, and N atoms. The $\mu_{\rm B}$ (−5.97 eV), $\mu_{\rm C}$ (−9.22 eV), and $\mu_{\rm N}$ (−8.32 eV) are the theoretical chemical potentials for B, C, and N atoms, which are

DOI:10.1063/1674-0068/27/04/394-398

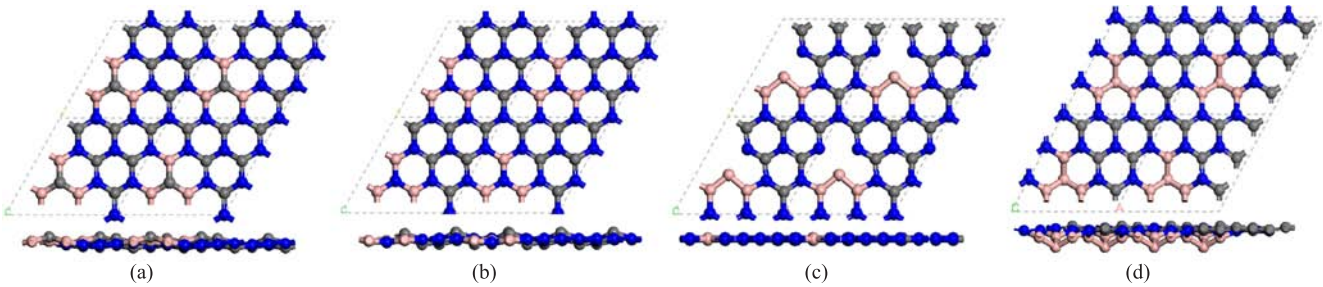

FIG. 2 The top (upper) and front (lower) views of (a) B_3C-C_3N_4, (b) B_3N-C_3N_4, (c) B_3-C_3N_4, and (d) B_4-C_3N_4. Gray, beige, and blue balls represent C, B, and N atoms, respectively.

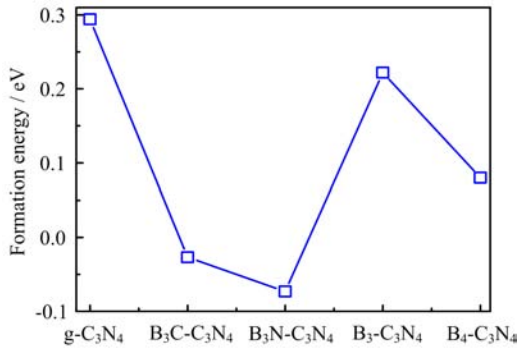

FIG. 3 The calculated average formation energy of pristine g-C_3N_4 and four B-C-N ternary monolayers.

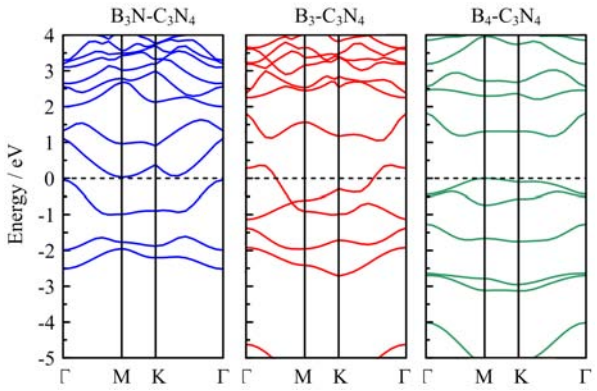

FIG. 4 The band structures of B_3N-C_3N_4, B_3-C_3N_4, and B_4-C_3N_4 are calculated with HSE06 method. The Fermi energy is set to be zero.

obtained from diamond boron phase, graphene and α-N_2 phase of gaseous nitrogen, respectively. The calculated average formation energy of pristine g-C_3N_4 and B-C-N ternary monolayer are summarized in Fig.3. It can be concluded that inserting B, C, or N atoms into the pores of g-C_3N_4 reduces its formation energy and these 2D B-C-N ternary monolayers are thermally stable. The B_3N-C_3N_4 sheet presents the highest stability in the considering systems, since the B−N bond has much higher bonding energy than B−C bond, which is consistent with the previous reports [8, 13]. The B_3-C_3N_4 and B_4-C_3N_4 systems show relatively low stability due to small bonding energy of B−B bond. The high thermal stability of B_3N-C_3N_4 and B_3C-C_3N_4 implies that they are the most probable structures to be formed in a synthesis process.

The electronic band structures of B-C-N ternary sheets are calculated within PBE and HSE06 funtional schemes. The calculations indicate that B_3N-C_3N_4, B_3-C_3N_4, and B_4-C_3N_4 sheets are nonmagnetic. The calculated energy band gaps and magnetic moment are summarized in Table I. Figure 4 displays the electronic band structures of B_3N-C_3N_4, B_3-C_3N_4, and B_4-C_3N_4 sheets. Different from pristine g-C_3N_4, the B_3N-C_3N_4 and B_3-C_3N_4 monolayers are metallic. The B_4-C_3N_4 semiconducts with an energy band gap of 1.18 eV, which is much smaller than that of pristine g-C_3N_4. The reduced band gaps of B_4-C_3N_4 indicate its advantages in the photocatalytic reaction.

However, the B_3C-C_3N_4 system is magnetic. In order to explore the magnetic ground state, ferromagnetic (FM), antiferromagnetic (AFM), and nonmagnetic (NM), configurations have been considered using a (2×2) supercell. It is found that the FM state is the most energetically stable, with energy of 36.47 and 37.29 meV lower than that of the AFM and NM configurations, respectively. The calculated magnetic moment is 0.57 μ_B/cell for a FM state. The calculated electronic band structure and spin charge density distribution profiles of B_3C-C_3N_4 system is displayed in Fig.5.

From Fig.5(a), it can be concluded that the magnetic moment of B_3C-C_3N_4 is mainly contributed by the carbon atoms in the system. When three boron atoms and one carbon atom are added into the porous of the pristine g-C_3N_4, three neighboring carbon atoms are spin polarized and the system becomes the metal-free magnetic material. Figure 5(a) also shows that the magnetic moment mainly comes from the $2p_z$ orbitals of the three neighboring carbon atoms and other atoms are slightly spin polarized. The calculated electronic band structures and atom-projected DOS (PDOS) (as shown in Fig.6(d)) analysis indicate there is strong spin-splitting for $2p_z$ orbitals of C atoms. Only one band crosses the

DOI:10.1063/1674-0068/27/04/394-398

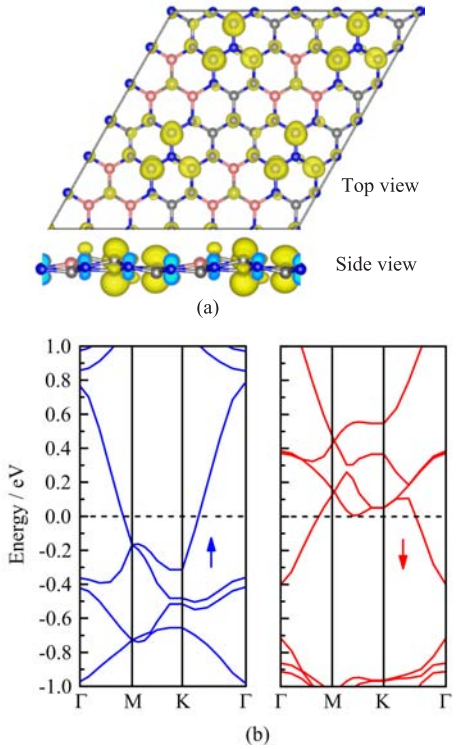

FIG. 5 (a) The top and side view of spin charge density of B_3C-C_3N_4. The isosurface is 0.002. (b) The electronic band structures are plotted for spin up and down channel with HSE06 method, respectively. The Fermi energy level is set to be zero.

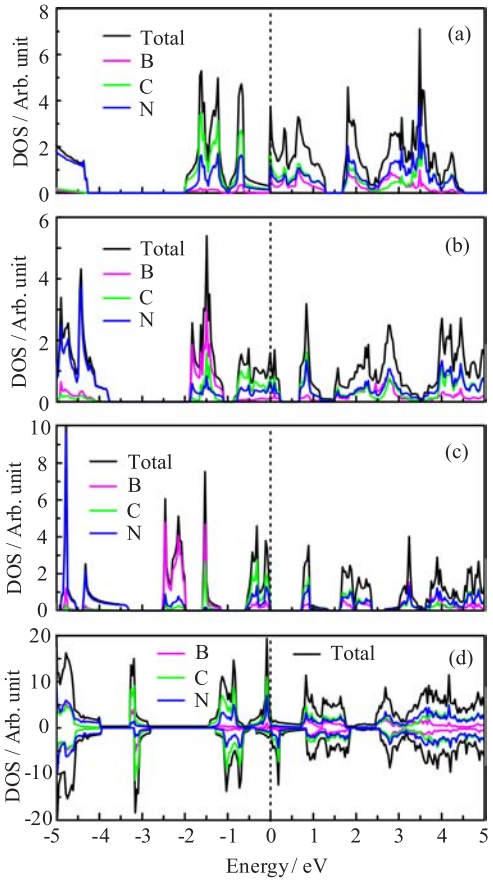

FIG. 6 The calculated DOS of (a) B_3N-C_3N_4, (b) B_3-C_3N_4, (c) B_4-C_3N_4, and (d) B_3C-C_3N_4. The Fermi energy level is set to be zero.

Fermi level monolithically in spin up and down channels, corresponding to the C2p_z orbitals. As mentioned above, for the pristine g-C_3N_4, the valence band edge is mainly contributed by N2p orbitals, whereas the conducting band edge is mainly contributed by C2p and N2p orbitals. However, for the B_3C-C_3N_4, as can be seen, the N2p states overlap significantly with those of C2p states near the Fermi level, suggesting a strong interaction between them, which results in the spin splitting of C2p_z orbitals. The magnetism characteristics of B_3C-C_3N_4 monolayer indicate its potential applications in spintronics devices.

For the nonmagnetic systems, Fig.6 displays the calculated PDOS with PBE method. The analysis of the PDOS demonstrates that, near the Fermi level, the most significant contribution for the charge transport in such systems are associated with the p orbitals of carbon and nitride while boron atoms make a little contribution due to only one electron in p orbital.

IV. CONCLUSION

In summary, we have proposed four B-C-N ternary sheets with uniform element distribution. It is demonstrated that all of the predicted new uniform B-C-N ternary systems are metals except the B_4-C_3N_4 which is a semiconductor with a band gap of 1.18 eV. Interestingly, B_3C-C_3N_4 is a metal-free ferromagnetic material and holds a magnetic moment of 0.57 μ_B/cell. The calculated formation energy indicates these B-C-N ternary sheets are highly thermal stable. Our studies present a method to design B-C-N ternary monolayer with uniform element distribution for electronic and spintronic applications.

V. ACKNOWLEDGMENTS

This work was supported by the National Key Basic Research Program (No.2012CB922001 and No.2011CB921404), the National Natural Science Foundation of China (No.21121003 and No.51172223), the Strategic Priority Research Program of CAS (No.XDB01020300), One Hundred Talent Program of CAS, the National Young Top Talent Program of Organization Department of China, the Fundamental Research Funds for the Central Universities (No.WK2060140014 and No.WK2060190025), and USTCSCC, SCCAS, Tianjin, and Shanghai Supercomputer Centers.

DOI:10.1063/1674-0068/27/04/394-398

[1] C. Lee, Q. Li, W. Kalb, X. Z. Liu, H. Berger, R. W. Carpick, and J. Hone, Science **328**, 76 (2010).
[2] K. S. Novoselov, D. Jiang, F. Schedin, T. J. Booth, V. V. Khotkevich, S. V. Morozov, and A. K. Geim, Proc. Natl. Acad. Sci. USA **102**, 10451 (2005).
[3] J. Zhou, Q. Wang, Q. Sun, and P. Jena, Phys. Rev. B **81**, 085442 (2010).
[4] E. Almahmoud, I. Kornev, and L. Bellaiche, Phys. Rev. B **81**, 064105 (2010).
[5] A. Nag, K. Raidongia, K. P. S. S. Hembram, R. Datta, U. V. Waghmare, and C. N. R. Rao, ACS Nano **4**, 1539 (2010).
[6] L. Song, L. Ci, H. Lu, P. B. Sorokin, C. Jin, J. Ni, A. G. Kvashnin, D. G. Kvashnin, J. Lou, B. I. Yakobson, and P. M. Ajayan, Nano Lett. **10**, 3209 (2010).
[7] A. V. Krasheninnikov, P. O. Lehtinen, A. S. Foster, P. Pyykkö, and R. M. Nieminen, Phys. Rev. L **102**, 126807 (2009).
[8] L. J. Ci, L. Song, C. H. Jin, D. Jariwala, D. X. Wu, Y. J. Li, A. Srivastava, Z. F. Wang, K. Storr, L. Balicas, F. Liu, and P. M. Ajayan, Nature Mater. **9**, 430 (2010).
[9] K. Raidongia, A. Nag, K. P. S. S. Hembram, V. U. Waghmare, R. Datta, and C. N. R. Rao, Chem. Eur. J. **16**, 149 (2010).
[10] L. Qin, J. Yu, S. Y. Kuang, C. Xiao, and X. D. Bai, Nanoscale **4**, 120 (2012).
[11] A. K. Manna and S. K. Pati, J. Phys. Chem. C **115**, 10842 (2011).
[12] S. Azevedo, Phys. Lett. A **351**, 109 (2006).
[13] A. Freitas, S. Azevedo, M. Machado, and J. R. Kaschny, Appl. Phys. A **10**, 1007 (2012).
[14] J. Y. Li, D. Q. Gao, X. N. Niu, M. S. Si, and D. S. Xue, Nanoscale Res. Lett. **7**, 624 (2012).
[15] M. S. C. Mazzoni, R. W. Nunes, S. Azevedo, and H. Chacham, Phys. Rev. B **73**, 073108 (2006).
[16] Y. J. Zhang, T. Mori, L. Niu, and J. H. Ye, Energy Environ. Sci. **4**, 4517 (2011).
[17] Y. J. Zhang, T. Mori, J. H. Ye, and M. Antonietti, J. Am. Chem. Soc. **132**, 6294 (2010).
[18] Q. J. Xiang, J. G. Yu, and M. Jaroniec, J. Phys. Chem. C **115**, 7355 (2011).
[19] X. D. Zhang, X. Xie, H. Wang, J. J. Zhang, B. C. Pan, and Y. Xie, J. Am. Chem. Soc. **135**, 18 (2013).
[20] D. Q. Gao, Q. Xu, J. Zhang, Z. J. Yang, M. S. Si, Z. L. Yang, and D. S. Xue, Nanoscale **6**, 2577 (2014).
[21] X. F. Chen, J. S. Zhang, X. Z. Fu, M. Antonietti, and X. C. Wang, J. Am. Chem. Soc. **131**, 11658 (2009).
[22] Z. X. Ding, X. F. Chen, M. Antonietti, and X. C. Wang, ChemSusChem **4**, 274 (2011).
[23] X. C. Wang, X. F. Chen, A. Thomas, X. Z. Fu, and M. Antonietti, Adv. Mater. **21**, 1609 (2009).
[24] M. Deifallah, P. F. McMillan, and F. Cora, J. Phy. Chem. C **112**, 5447 (2008).
[25] A. Du, S. Sanvito, Z. Li, D. W. Wang, Y. Jiao, T. Liao, Q. Sun, Y. H. Ng, Z, H. Zhu, R. Amal, and S. C. Smith, J. Am. Chem. Soc. **134**, 4393 (2012).
[26] J. P. Perdew, K. Burke, and M. Ernzerhof, Phys. Rev. Lett. **77**, 3865 (1996).
[27] G. Kresse and J. Furthmuller, Phys. Rev. B **54**, 11169 (1996).
[28] P. E. Blochl, Phys. Rev. B **50**, 17953 (1994).
[29] G. Kresse and D. Joubert, Phys. Rev. B **59**, 1758 (1999).
[30] H. J. Monkhorst and J. D. Pack, Phys. Rev. B **13**, 5188 (1976).
[31] X. C. Wang, K. Maeda, A. Thomas, K. Takanabe, G. Xin, J. M. Carisson, K. Domen, and M. Antonietti, Nat. Mater. **8**, 76 (2009).

DOI:10.1063/1674-0068/27/04/394-398